PERIODICA POLYTECHNICA SER. MECH. ENG. VOL. 41, NO. 1, PP. 3-20 (1997)

INVESTIGATION OF LOADED FIBROUS FILTER

Abd El-Hamied Abdoh ABD EL-HAMIED and Tamás LAJOS

Department of Fluid Mechanics
Technical University of Budapest
H-1521 Budapest, Hungary

Received: July 3, 1996

Abstract

This paper presents results of theoretical and experimental investigations of the effect of dust deposition on filter performance. In the theoretical model, the filter is divided into elements of various structural characteristics and the effect of fibers and deposited particles on pressure drop and collection efficiency is considered. In the suggested model, the part of the deposited particles increases the diameter of fibers, the rest form dendrites. Two dimensional flow fields in inhomogeneous filter mat are described by the continuity equation and Darcy equation. In order to obtain a clear idea about the effect of dust load on pressure drop and filter efficiency experimental investigations of clogging process in filter mats were performed where the temporal change of pressure drop and grade efficiency were measured. Theoretical and experimental results indicate that due to deposited particles the collection efficiency of filters increases rather rapidly with loading because the previously deposited particles offer additional collection surface. Deposited particles increase also the pressure drop across the filter by additional drag to gas flow. Calculations of streamlines through inhomogeneous filter mat indicate that deposited particles increase the uniformity of the flow field. The comparison of the results of calculation and experimental data on temporal change of collection efficiency and pressure drop shows considerable agreement.

Keywords: fibrous filter, clogging process, inhomogeneity, deposited particles, collection efficiency, pressure drop, flow field.

1. Introduction

At present time with increase of generation of air pollutants from various sources such as motors of vehicles, cement furnace, asphalt plants, coal fired boilers, etc., the demand for filters is increasing for protecting both human life nature and equipment in manufacture and use.

Filter performance for a particular application may be characterized by three factors: (i) the collection efficiency of the clean filter. (ii) initial air flow resistance, and (iii) change of efficiency and resistance of filter due to accumulation of particles during the clogging process. The collection efficiency and pressure drop of clean filters can be calculated from the

conventional theories but no efficient method for prediction of the effect of dust load on pressure drop and filter efficiency is available.

Efforts were made by [1,2,3,4,5] to determine the effect of dust deposition on pressure drop and filter efficiency and to simulate the clogging process in fibrous filters. These methods describe the very complicated process of filter clogging by neglecting a number of more or less influencing factors, so they can be expected to give qualitatively correct results only. The deposited particles that form dendrites become effective from the point of view of increase of pressure drop and collection efficiency [3,4]. Single fiber efficiency is a very important parameter in calculation of the filter efficiency and change of the particle concentration in filter mat. Therefore, several researchers tried to consider the effect of loading by modifying on the single fiber efficiency [6,7,8,9]. Most of authors [7,8,9] reported that the ratio between the single fiber efficiency for loaded filter and that for clean filter can be approximated by a linear function of concentration of deposited particles as follows:

$$\frac{\eta_l}{\eta_f} = 1 + \lambda c_d \tag{1}$$

Theoretical and experimental studies have been made [10] on the effect of deposited mono and polydisperse particles on the single fiber efficiency for uncharged fibers. It was observed that single fiber efficiency increases linearly for monodisperse particles, whilst exponentially for polydisperse particles during clogging process. There are numbers of papers describing the change of total collection efficiency during clogging for monodisperse, but rather fractional collection efficiency $T(d_p)$ for polydisperse particles [11,12]. LAJOS [13,14] proposed a model for calculation of flow field in inhomogeneous filter bed as well as a simplified one-dimensional calculation of the change of filtration efficiency and pressure drop during filtration process. SCHWEERS and LÖFFLER [15] studied the effect of filter structural inhomogeneities on pressure drop and collection efficiency of clean filter mats. LAJOS and ABD EL-HAMIED [16] proposed a method for calculation of change of collection efficiency and pressure drop through a filter mat during clogging process using several simplified models.

2. Theory

2.1 Particle Deposition Balance

The rate of accumulated particles ($\frac{c_d}{\Delta_t}$) in a filter element of thickness Δx and flow area ($\Delta y x 1$) can be derived from balance of mass of particles for

a filter element. The mass balance equation for a control volume, *Fig. 1*, is as follows:

$$\frac{c_d}{\Delta t} = -\Big(\frac{(J_s - J_n}{\Delta x)} + \frac{(J_e - J_w)}{\Delta y}\Big), \tag{2}$$

where J is the mass flux and equal to $c|\mathbf{v}|$.

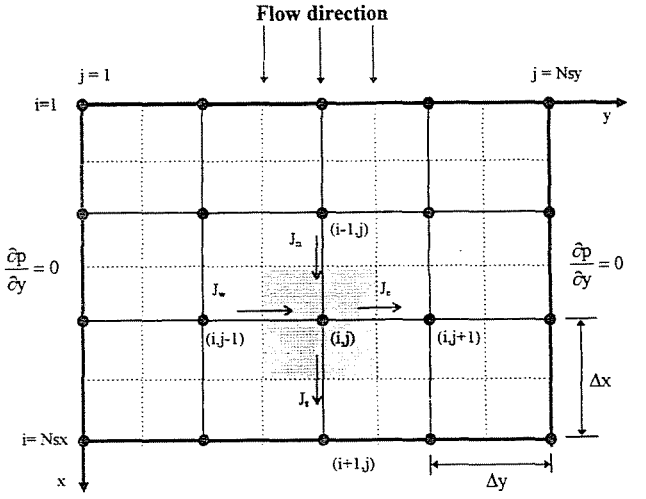

Fig. 1. Grid notation, control volume, nodal location, staggered location

2.2 Effect of Particle Deposition on Pressure Drop

Particle deposition affects the pressure drop to great extent. In order to approximate the complicated process of particle deposition a model has been developed combining two types of deposition. A part of the particles forms a layer on the surface of the fibers increasing in this way their diameter from d_f to d_{th} (thickening model). The rest of deposited particles forms dendrites that can be considered as additional fibers of diameter d_p. We suppose that at the beginning of filtration process the former mechanism prevails, later more and more particles form dendrites. Consequently the share of particles participating in thickening the fibers or forming dendrite depends on the concentration of the deposited particles.

The dust particles deposited on fibers or on particles separated previously increase the total surface of fibers and particles in filter element. We assume that the surface of fibers and collected particles determines the collection surface playing important role in the particle separation. It has to be considered that the increase of the collecting surface is smaller than the

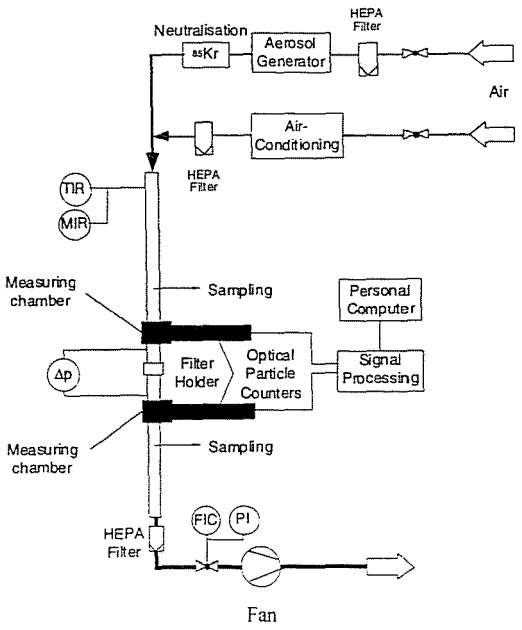

Fig. 2. Schematic diagram of the experimental set-up
TIR Instrument for measuring temperature
MIR Instrument for measuring humidity
FIC Instrument for measuring air flow
PI Instrument for measuring pressure

surface of deposited particles, since the particles and fibers and particles and particles partially shade each other. The relation between concentration of deposited particles c_d and specific collecting surface of deposited particles, a_c (m^2/m^3), of diameter d_p is (3)

$$c_d = \frac{a_c \cdot d_p \rho_p}{6k}$$

where the value of k constant, expressing the shadowing effect, is smaller than unity. Using the method proposed in [14], the pressure drop through a filter mat section of thickness Δx equals the drag forces acting on all fibers and dendrites of unit area of filter mat

$$\Delta p = F(L_{th} + L_{den}), \tag{4}$$

where F is the drag force per unit length

$$F = \mu v F^*. \tag{5}$$

In the calculations the Kuwabara model [17] has been applied, that has proved to be a good approximation of the relation between pressure drop and flow velocity in the filter mat. According to this method the dimensionless drag coefficient F^*

$$F^* = \frac{4\pi}{Ku}, \tag{6}$$

where

$$Ku = -0.5 \ln \alpha - 0.75 + \alpha - 0.25\alpha^2$$

and α is the total packing density [17].

L_{th} is the thickened fiber length and L_{den} is the dendrite length per unit area of a filter element of thickness Δx [18].

L_{th} is equal to the fiber length and L_{den} can be expressed by knowing a_{den}, the specific surface of particles forming dendrites; $L_{den} = \frac{a_{den}\Delta x}{\pi d_p}$.

According to Darcy equation the pressure drop across porous layer is directly proportional to velocity through them. The generalized form of Darcy equation is

$$\mathbf{v} = -C \operatorname{grad} p, \tag{7}$$

where C is the permeability coefficient. From *Eqs.* (2-7), the permeability coefficient is

$$C = \frac{Ku}{4\mu\left(\frac{a_{th}}{d_{th}} + \frac{a_{den}}{d_p}\right)}. \tag{8}$$

In the combined model proposed by the authors, the share of deposited particles forming dendrite is expressed by factor b representing the ratio of dendrite packing density to total packing density of deposited particles [15].

$$\Delta\alpha_{den} = b\Delta\alpha_d, \tag{9}$$

where $\Delta\alpha_d$ is the deposited particles packing density, $\Delta\alpha_d = \frac{c_d}{\rho_p}$.

The length of thickening fiber per unit volume equals the length of fibers in clean filter, thus, and using the relation between the specific surface and packing density, the permeability coefficient *Eq.* (8) becomes

$$C = \frac{Ku}{16\mu\left(\frac{\alpha_f}{d_f^2} + \frac{bc_d}{\rho_p d_p^2}\right)}. \tag{10}$$

2.3 Flow Field

The inhomogeneity of filter structure influences the flow field in filter mats and the separation of aerosol particles from dusty gases [13]. Also, the deposited particles contribute to inhomogeneity of packing density in fibrous filters and change continuously the flow field during the clogging process. In calculation of the flow field in filter mat the effect of fibers and deposited particles are taken into consideration. Furthermore, it is assumed that gas flow in the filter obeys Darcy equation the e.g. the inertia term of the momentum equation can be neglected and gas density is constant. Neglecting the displacement effect of fibers and deposited particles the continuity equation for incompressible gas is

$$\operatorname{div} \mathbf{v} = 0. \tag{11}$$

Substituting *Eq.* (7) in *Eq.* (11), and assuming a $2D$ flow field, the following equation for the pressure distribution in a filter mat is obtained

$$\frac{\partial p}{\partial x}\left(C\frac{\partial}{\partial x}\right)\frac{\partial}{\partial y}\left(\frac{\partial}{\partial y}\right) = 0. \tag{12}$$

In accordance with the condition that the pressure is constant at the inlet and outlet and no flow may pass through the periphery of the filter section *Fig. 1*, boundary conditions for pressure are at

$$\begin{aligned} &x = 0, && p = p_{in}, \\ &x = h, && p = p_{in} - \Delta p, \\ &y = 0 \quad \text{and} \quad && y = nsy\ \frac{\partial p}{\partial y} = 0. \end{aligned} \tag{13}$$

The velocity component can be deduced as follows:

$$\begin{aligned} v_x &= -C\frac{\partial p}{\partial x} = \frac{\partial \Psi}{\partial y}, \\ v_y &= -C\frac{\partial p}{\partial y} = -\frac{\partial \Psi}{\partial x}, \end{aligned} \tag{14}$$

where Ψ [m^2/s] is the stream function.

2.4 Concentration Field and Filter Efficiency

Knowing the flow field through filter mat and the element separation efficiency, concentration of suspended particles in the flow can be calculated. The element separation efficiency $\eta_{(i,j)}$ is calculated using the conventional theory with regarding as first approximation the single fiber efficiency for loaded filter, *Eq.* (1), and the original fiber surface. (In this case the formation of dendrites and thickening of fibers are considered of calculation of flow field and pressure drop.)

The numerical procedure starts by determining the pivot elements in every row of filter grid. The pivot element is an element, all inlet concentration and flow velocity components are known. Particle concentration leaving that elements are firstly calculated and after that rest of row elements. Particle concentration leaving each element can be calculated from the following equation [15]:

$$c_{o(i,j)} = c_{i(i,j)}(1 - \eta_{(i,j)}), \tag{15}$$

where $c_{i(i,j)}$ is inlet concentration of particles that equals the ratio of all inlet mass flow rates and all inlet flow rates to the element.

The outlet concentration and the separation efficiency for the filter mat is calculated as follows;

$$c_{o(filter)} = \frac{\sum_{j=1}^{j=nsy} c_{o(nsx,j)} V_{x(nsx,j)} \Delta y}{\sum_{j=1}^{j=nsy} V_{x(nsx,j)} \Delta y}, \tag{16}$$

$$E = 1 - \left(\frac{c_0}{c_i}\right)_{\text{filter}}. \tag{17}$$

The differential equation (12) with the boundary conditions, *Eq.* (13), is solved using finite volume differencing method [19]. Pressure field is computed at the main nodal locations, while velocities are determined at staggered locations, *Fig. 1.* Particle deposition is also calculated taking the flow field and the separation effect of the fibers, and the deposited particles into consideration.

3. Experimental Investigation

Experiments have been performed to investigate the clogging process in filter mats. The experimental set-up, designed and manufactured in *Institut*

für Mechanische Verfahrenstechnik und Mechanik in Karlsruhe University Germany, Fig. 2, consists of three main parts: the aerosol generator, the flow channel with two measuring chambers and the actual measuring unit. Aerosol generator used to disperse powder consists of a rotating brush and pressurised air flow to disperse definite amount of powder at a highly constant rate. After the aerosol generator a ^{85}Kr-source (10 mci) as an aerosol neutraliser is installed because the particles carry generally high electrical charges after the initial aerosol generation process. Particle concentration can be varied in a wide range by adjusting the generator and mixing air flow. After the mixing chamber aerosol is directed in a tubular flow channel of inner diameter 50 mm. At the inlet of the flow channel the air temperature (TIR) and relative humidity (MIR) can be monitored. The aerosol flows towards the filter holder that holds the test filter, the diameter of which is 52 mm and a thickness of up to 2.5 cm depending on the filter media. Dust particles penetrating the test filter were captured perfectly by a backup HEPA filter. Behind the backup filter the air flow is monitored by a rotameter and pressure transducer and controlled by a pump (FIC, PI). The face velocity of the test filter can be altered and adjusted in the range from 0.1 to 2.0 m/s, which is typical for filter media used in air conditioning systems. The size and flux of particles upstream and downstream of the test filter are measured using two identical optical particle counters that operate with optically defined measuring volumes allowing direct measurement in the pipe flow, *Fig. 2*. Each measuring volume is situated at the center of the chamber cross section. Several dimensions for the cross section areas of the measuring volumes were chosen to reduce the difference in particle counting rates of the optical particle counters, because the downstream concentration is much lower than the upstream concentration. The scattered light signals of both optical particle counters are amplified and evaluated by a special computer program on a PC that collects and processes the data. The filter pressure drop was measured, using pressure taps installed upstream and downstream of the filter, by a differential pressure gauge.

The filtration process is traditionally characterized by grade or fractional efficiency $T(d_p)$ that can be expressed as a function of particle size d_p and other operating parameters

$$T(d_{pi}) = 1 - \frac{J_o(d_{pi})}{J_i(d_{pi})}, \tag{18}$$

where the subscripts i and o mean inlet and outlet conditions, d_{pi} is the mean particle size of i-th size interval and $J(d_{pi})$ is the particle flux.

4. Results

In this chapter theoretical and experimental results on the effect of dust load on the filter characteristics will be discussed and comparison between theoretical and experimental results is made.

To study the effect of inhomogeneity of filter structure, firstly, we assumed that a filter is composed of two parts of initial packing densities α_1 and α_2. Numerical simulations of clogging process have been carried out by changing the ratio of these parts expressed by y_1 which is the ratio from the cross sectional area A_1 characterized by packing density α_1 to the total cross sectional area of the filter A as shown in *Fig. 3a*. *Fig. 3b* illustrates the effect of y_1 on the pressure drop and filter efficiency at constant mean filtration velocity. *Fig. 3b* indicates that pressure drop and filter efficiency increase with increasing y_1, i.e. the relative area of filter part of higher packing density at given filter load. This is due to the fact that the permeability coefficient decreases with increase of the packing density and consequently the pressure drop rises. Increasing the relative area y_1 causes an increase of collection surface that raises filter efficiency. The change of filtration velocities in both parts of the filter during the clogging process can be seen in *Fig. 3c*. From this figure we can see a relatively high velocity through the part of low packing density (high permeability) whereas a lower velocity through the part of higher packing density. The filtration velocity through the low packing density part of the filter decreases while in the high packing density part it increases with increasing dust load until they reach the mean flow velocity v_m. At a given dust load we can notice that filtration velocity in both parts of the filter decreases with increasing the relative flow area y_1. This calculation indicates that low packing density filter elements like pinholes can influence considerably the overall operation of the filter.

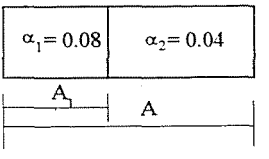

Fig. 3a. Filter structure; $y_1 = A_1/A$

Fig. 4 shows an example of clogging process calculations for regular 2D distribution of packing density, shown in *Fig. 4a*, at constant mean filtration velocity. Solid lines in *Fig. 4b* show the streamlines at clean filter, $m_p = 0$, while dashed lines indicate the streamlines at different dust loads. In *Fig. 4c* the velocity distributions at $x = 0$ and $x = h$ can be

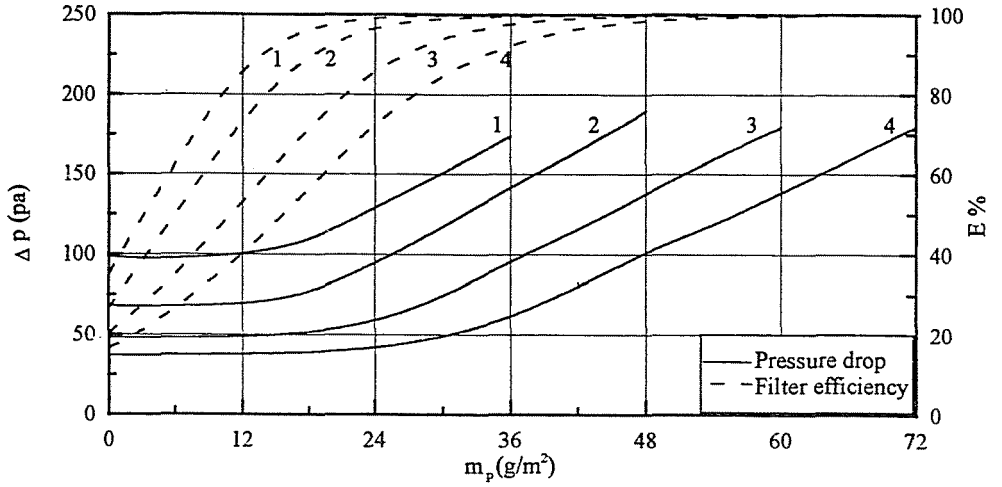

Fig. 3b. Computed pressure drop and filter efficiency at different values y_1 ($1 : y_1 = 1$; $2 : y_1 = 0.75$; $y_1 = 0.5$; $4 : y_1 = 0.25$)

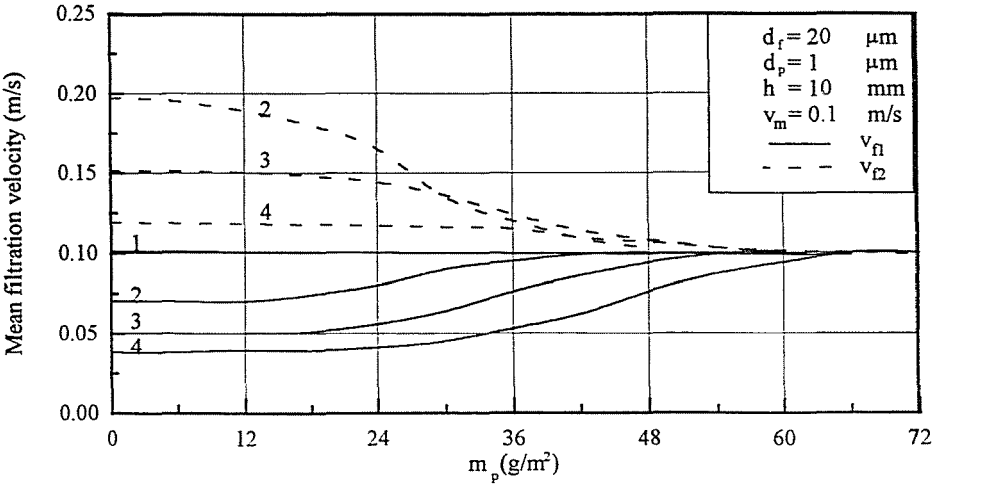

Fig. 3c. Computed filtration velocity in two parallel paths at different values y_1 ($\rho_p = 2000\text{kg/m}^3$, $\mu = 1.810^{-5}$ kg/m s)

seen. A large part of the gas flows with a relatively high velocity through regions of low packing density, and the other part of the flow passes with lower velocity through the regions of higher packing density. The change of inlet and outlet velocity with increasing dust load reflects the effect of deposited particles on the permeability coefficient and consequently on the flow field, *Fig. 4c*. At a given dust load, the pressure drop falls significantly

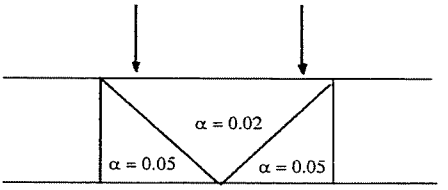

Fig. 4a. Filter structure

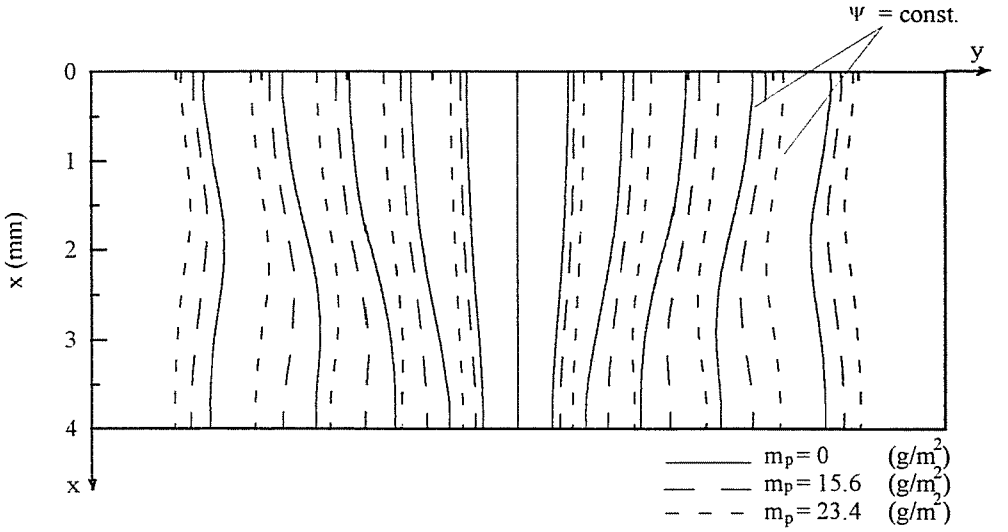

Fig. 4b. Streamlines through filter mat

with increasing the inhomogeneity of the filter mat (see *Fig. 4d*) since the inhomogeneity of packing density leads to an inhomogeneity of local permeability causing a higher total permeability. It is seen from *Fig. 4d* that the filter efficiency at constant packing density is greater than at changing packing density distribution.

Most real filters can be simulated by randomly distributed packing density of filter mat. The numerical simulation of clogging process: all fibers in the filter were assumed as identical and parallel. The packing density distribution of filter elements is randomly selected from Gaussian distribution. The number of elements versus different values of packing density at $\sigma/\alpha = 0.2$ is shown in *Fig. 5a*. The temporal change of pressure drop and filter efficiency at different values of relative standard deviation (σ/α) is shown in *Fig. 5b*. From this figure, it can be seen that pressure drop

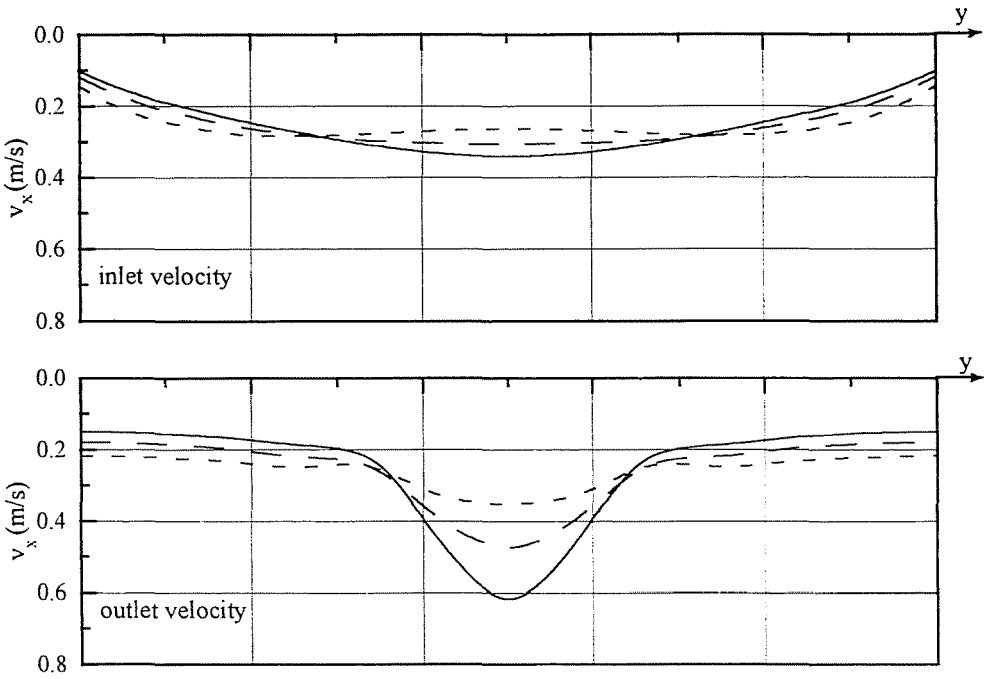

Fig. 4c. Change of v_x at inlet and outlet of filter mat

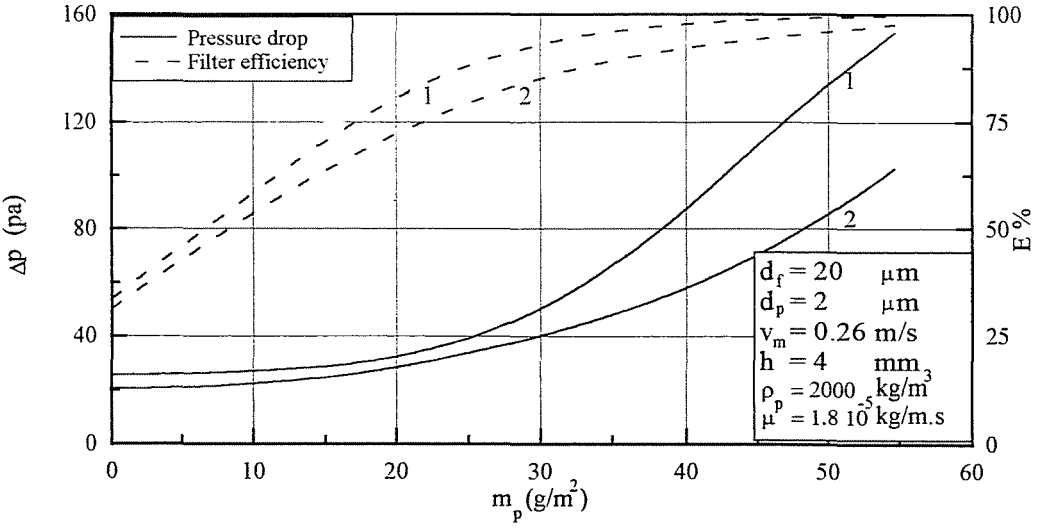

Fig. 4d. Change of pressure drop and filter efficiency(1:$\alpha_m = 0.035$; 2:inhom.filter)

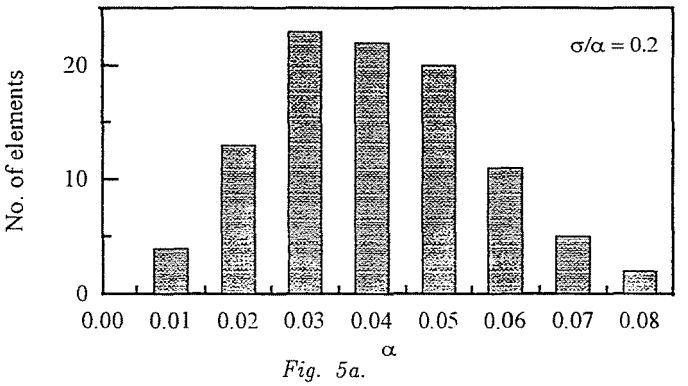

Fig. 5a.

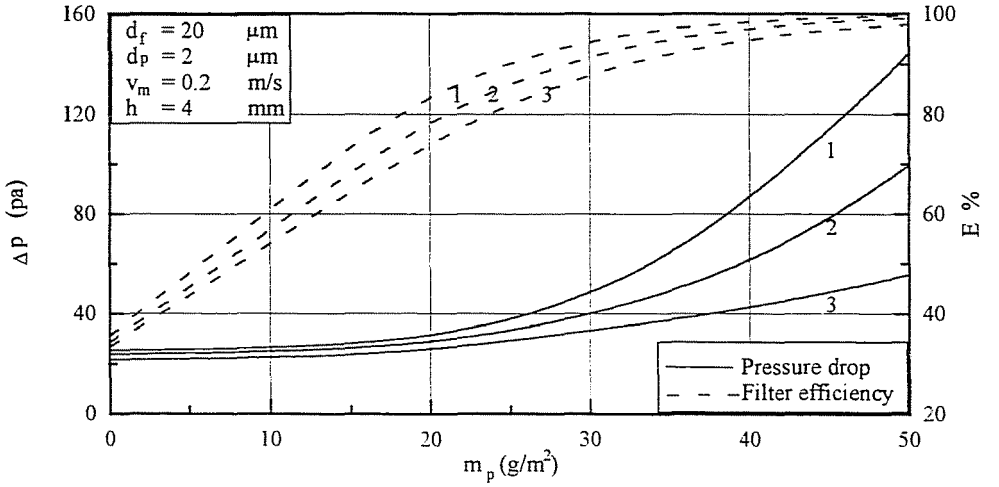

Fig. 5b. Computed results for the pressure drop and filter efficiency at different values of σ/α, ($1 : \alpha_m = 0.04$, $2 : \sigma/\alpha = 0.2$, $\sigma/\alpha = 0.3$)

and filter efficiency decrease with increasing the value of (σ/α) at constant load. Reductions in pressure drop due to the permeability of filter mat increases with increasing the inhomogeneity of the filter characterised by the relative standard deviation of the packing density distribution [13]. The inhomogeneity of packing density distribution causes decrease in collection efficiency a result of its influence on the flow characteristics and collecting surface in filter mat. This reduction in collection efficiency increases with

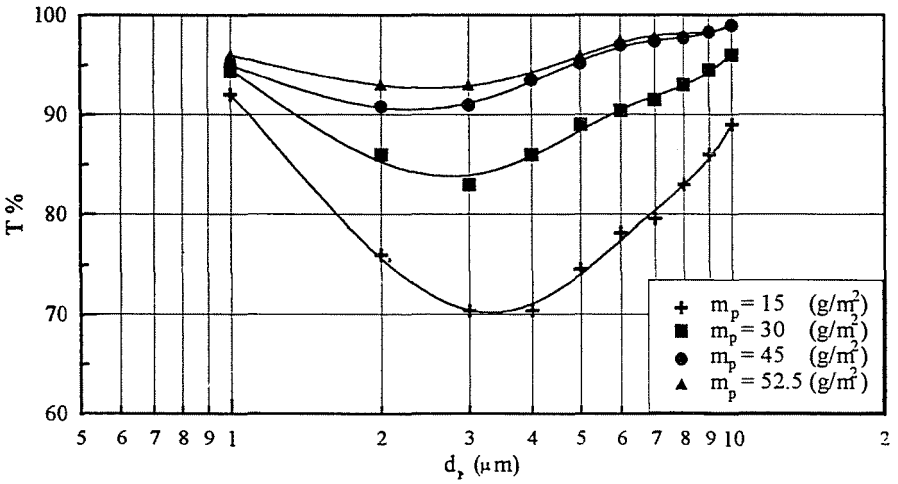

Fig. 6. Effect of incoming mass of particles on grade efficiency

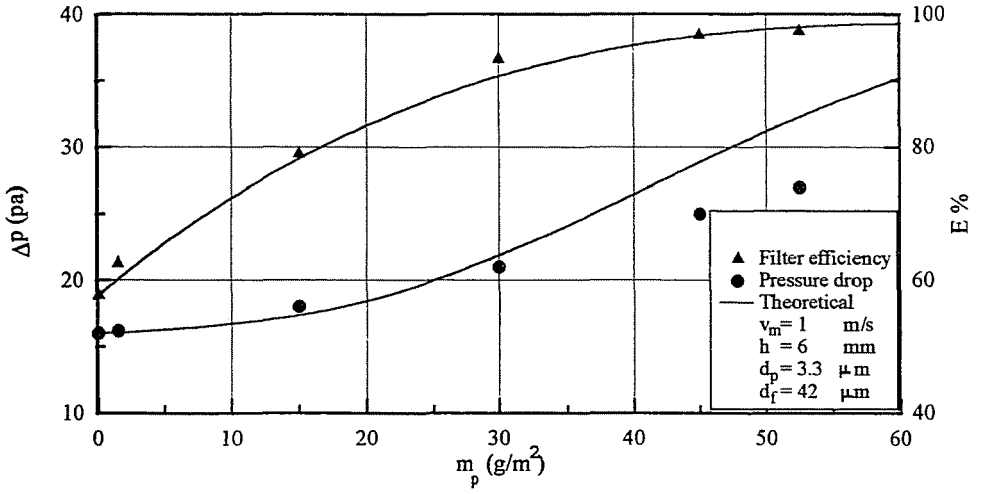

Fig. 7. Comparison between theoretical and experimental results

creasing the relative standard deviation of packing density as shown in ig. 5b.

Fig. 6 indicates the change of measured grade efficiency of the filter th particle size at different filter load. It can be seen that grade efficiency

decreases with increasing particle size up to 3 μm because the diffusion collection decreases with increasing particle size. For particle size range from 3 μm to 11 μm, the grade efficiency increases because the inertial deposition and interception are more effective and the diffusion can be neglected. Furthermore, it can be observed that the grade efficiency increase considerably with increasing dust load because the deposited particles increases the collection surface and collect more particles from the dusty gas.

Fig. 7 shows the comparison between the experimental and the theoretical results for the pressure drop and filter efficiency as a function of incoming mass of particles. The theoretical results have been obtained based on the combined model, by using the share factor as a linear function of the concentration of deposited particles, $b= 0.02375\ c_d$, [19] with the following constant parameters: initial packing density $\alpha = 0.02$, dust concentration in incoming gas $c = 500$ mg/m^3 and density of particles 2710 kg/m^3. The initial single fiber efficiency is calculated from the clean filter efficiency by using the conventional filtration theory. The clean filter efficiency is extrapolated from the first and second measurements 1 and 5 min. from beginning of filter loading. The figure shows that the deposition of solid particles on fibrous filters causes an increase in the filter efficiency and pressure drop. Furthermore, it can be seen from this figure that the rate of increase in filter efficiency is higher at the initial stages, then becomes smaller in the later stages of loading. In the initial stages of filter loading, the deposited particles protrude from the fiber surface hence provide a new surface area and in the given cross section the limiting streamlines move farther away from the fiber surface [20]. As a result, deposited particles have a greater chance to collect oncoming particles than an equivalent fiber surface area and a single fiber efficiency rises. While in the last stages of filter loading, the newly deposited particles adhere to the particles deposited earlier and form new layers without considerable increase of collecting surface. In contrast, the change of the pressure drop in the initial stage of loading is small and in the final stage is rapid. The above behaviour due in the initial stage, to, the amount of deposited particles is small and the particles increase the fiber diameter (thickening model) consequently, its contribution to the filter resistance is small. But in the high loading region the contribution of the deposited particles to the resistance is high due to dendrite formation. The deviation between the theoretical and experimental results may be due to the inhomogeneity effects of the test filter that requires more thorough experimental investigation to know the macroscopic structure of the test filter. Another reason for this deviation is that calculation monodisperse particles were assumed but in the experiments polydisperse particles were used.

5. Conclusions

The main conclusions from this study are:

i) The inhomogeneity in the filter structure plays an important role in the change of the pressure drop and the filtration efficiency during the clogging process.

ii) At a given dust load, the filter efficiency and pressure drop through a filter mat having regular or randomly distributed packing density is smaller than that having uniform packing density corresponding to the mean packing density.

iii) The combined model is a suitable approximation in the calculation of pressure drop during clogging process.

Acknowledgment

The authors are grateful to Dr. E. Schmidt and Mr. R. Maus for their fruitful helping in performing the experiments. The authors would also like to acknowledge the Cultural Bureau of the Egyptian Embassy in Budapest, Technical University of Budapest and OTKA for supporting this work.

Nomenclature

a_c	Specific collecting surface [m^2/m^3]
A	Filter cross sectional area [m^2]
b	Share factor [−]
c	Particle concentration [kg/m^3]
C	Permeability coefficient [$m^4/N.s$]
d	Diameter [m]
E	Filter efficiency [−]
F	Drag force per unit length [N/m]
F^*	Dimensionless drag [−]
h	Filter thickness [m]
J	Mass flux [$kg/m^2.s$]
k	Constant, *Eq.* (3), ($k = 0.5$) [−]
L	Fiber length per unit area [m/m^2]
m_p	Dust load [g/m^2]
p	Pressure [Pa]
t	Time [s]
T	Grade efficiency [−]
$\mathbf{v}$	Velocity vector [m/s]
v_x	Velocity component in x direction [m/s]

v_y	Velocity component in y direction [m/s]
y	Relative area [−]
Δ_x	Thickness of filter element [m]
Δ_y	Width of control volume in y direction [m]

Greek Letters

α	Packing density [−]
λ	Raising factor [m^3/kg]
μ	Dynamic viscosity [kg/m.s]
ρ	Density [kg/m^3]
σ	Standard deviation [−]
η	Single fiber efficiency [−]
Ψ	Stream function [m^2/s]

Subscripts

d	Deposited
den	Dendrite
f	Fiber, filtration
i	Inlet condition
l	Loaded condition
m	Mean value
o	Outlet condition
p	Particle
th	Thickening

References

1. STENHOUSE, J. I. T. – TROTTIER, R. (1991): The Loading of Fibrous Filters with Submicron Particles, *J. Aerosol Sci.* Vol. 22, pp. S777–S780.
2. YOSHIOKA, N. et al. (1969): Filtration of Aerosols Through Fibrous Packed Bed with Dust Loading, *Chem. Eng. Japan*, Vol. 33, pp. 1013–1019.
3. KANAOKA, C. et al. (1980): Simulation of the Growing Process of Particle Dendrite and Evaluation of a Single Fiber Collection Efficiency with Dust Load, *J. Aerosol Sci.* Vol. 11, pp. 377–389.
4. BERGMAN, W. et al. (1976): Enhanced Filtration, Lawrence Livermore Laboratory.
5. HAMPTON, J. H. D. – SAVAGE, S. B. (1993): Computer Modeling of Filter Pressing and Clogging in a Random Tube Network, *Chem. Eng. Sci.* Vol. 48, pp. 1601–1611.
6. LASTOW, O. (1994): Simulation of Dendrite Formation of Aerosol Particles on a Single Fibre, *J. Aerosol Sci.* Vol. 25, pp. S199–S200.
7. MYOJO, T. et al. (1984): Experimental Observation of Collection Efficiency of a Dust–Loaded Fiber, *J. Aerosol Sci.* Vol. 15, No. 4, pp. 483–489.

8. STENHOUSE, J. et al. (1992): The Behaviour of Fibrous Filters in the Initial Stages of Filter Loading, *J. Aerosol Sci.* Vol. 23, pp. S761–S764.
9. BILLINGS, C. E. (1966): Effect of Particle Accumulation in Aerosol Filtration, Ph.D. Thesis, California Institute of Technology, Pasadena.
10. BAUMGARTNER, H. – LÖFFLER, F. (1987): Three-dimensional Numerical Simulation of the Deposition of Polydisperse Aerosol Particles on Filter Fibres, Extended Concept and Preliminary Results, *J. Aerosol Sci.* Vol. 18, pp. 885–888.
11. UMHAUER, H. et al. (1990): Measuring Filter Efficiency by Optical High Concentration (HC) Single Particle Analyser, *Filtration & Separation,* May/June, pp. 188–191.
12. MAUS, R. – UMHAUER, H. : Determination of the Fractional Efficiencies of Fibrous Filter Media by Optical In-Situ Measurements, private communication.
13. LAJOS, T. (1985): The Effect of Inhomogeneity on the Flow in Fibrous Filters, *Staub Reinhaltung der Luft*, Band 45, pp. 19–22.
14. LAJOS, T. (1986): A Model for Calculation of Clogging Process in Filter Mats, *1. World Congress Particle Technology Nürnberg*, pp. 175–188.
15. SCHWEERS, E. – LÖFFLER, F. (1994): Realistic Modelling of the Behaviour of Fibrous Filters through Consideration of Filter Structure, *Powder Technology* Vol. 80, pp. 191–206.
16. LAJOS, T. – ABD EL-HAMIED, A. A. (1995): Simulation of The Clogging Process in Filter Mats, *3rd. European Symposium, Separation of Particles from Gases*, Nürnberg, Germany, 21-23 March, pp. 243–252.
17. KUWABARA, S. (1959): The Forces Experienced by Randomly Distributed Parallel Circular Cylinders or Spheres in Viscous Flow at Small Reynolds Numbers, *J. Phys. Soc.* Japan Vol. 4, pp. 527–532.
18. ABD EL-HAMIED, A. A. et al. (1996): Effect of Particle Deposition on the Flow through Fibrous Filters, *International Symposium Filtration and Separation of Fine Dust*, Vienna, Austria, April 24-26, pp. 114–125.
19. PATANKAR, S. V. (1980): Numerical Heat Transfer and Fluid Flow, McGraw-Hill, New York.
20. TIEN, C. et al. (1977): Chainlike Formation of Particle Deposits in Fluid-Particle Separation, *Science* Vol. 196, pp. 983–985.